Journal of Applied Polymer Science

Effect of surfactant and electron treatment on the electrical and thermal conductivity as well as thermal and mechanical properties of ethylene vinyl acetate/expanded graphite composites

Jeremia Shale Sefadi,[1] Adriaan Stephanus Luyt,[1*] Jürgen Pionteck,[2] Francesco Piana,[2,3†] Uwe Gohs[2]

[1]Department of Chemistry, University of the Free State (Qwaqwa Campus), Private Bag X13, Phuthaditjhaba 9866, South Africa
[2]Leibniz-Institut für Polymerforschung Dresden e.V., Hohe Str. 6 01069 Dresden, Germany
[3]Technische Universität Dresden, Organic Chemistry of Polymers, 01062 Dresden, Germany
*Present address: Center for Advanced Materials, Qatar University, PO Box 2713, Doha, Qatar
†Present address: Institute of Macromolecular Chemistry, AV ČR, v. v. i., Heyrovského nám. 2, 162 06 Prague 6, Czech Republic
Correspondence to: A. S. Luyt (E-mail: aluyt@qu.edu.qa or LuytAS@qwa.ufs.ac.za)

ABSTRACT: This study presents an investigation of the electrical and thermal conductivities of composites based on an ethylene vinyl acetate (EVA) copolymer matrix and nanostructured expanded graphite (EG). To improve the EG dispersion in EVA, EG sheets were modified by treating them with the anionic surfactant sodium dodecyl sulphate (SDS) in water. The modified SDS-EG platelets, after being filtered and dried, were melt-mixed with EVA to prepare the composites. Finally, both EVA/EG and EVA/SDS-EG composites were subjected to 50 kGy electron beam (EB) irradiation. SEM images confirm that the irradiated EVA/EG samples had improved interfacial adhesion, while the irradiated EVA/SDS-EG samples showed even better interfacial adhesion. The gel contents of the irradiated samples without and with SDS treatment increased with increase in EG loading. The EVA/EG composites exhibited a sharp transition from an insulator to a conductor at an electrical percolation threshold of 8 wt %, but with SDS-EG the electrical conductivity was extremely low, showing no percolation up to 10 wt % of filler. The EB irradiation had no influence on electrical conductivity. The thermal conductivity linearly increased with EG content, and this increase was more pronounced in the case of SDS-EG, but decreased after EB irradiation. The thermal properties were little influenced by EB irradiation, while better polymer–filler interaction and better filler dispersion as a result of SDS treatment, and the EB irradiation initiated formation of a cross-linked network, had a positive effect on the tensile properties. © 2015 Wiley Periodicals, Inc. J. Appl. Polym. Sci. **2015**, *132*, 42396.

KEYWORDS: composites; cross-linking; irradiation; properties and characterization

Received 2 October 2014; accepted 20 April 2015
DOI: 10.1002/app.42396

INTRODUCTION

Conventional polymers are materials possessing low thermal and no electrical conductivities, and these primarily depend on the extent of crystallinity. However, there are many industrial applications such as circuit boards, heat exchangers, electromagnetic shielding devices, antistatic plastics, packaging, and others that require an improvement in both the thermal and electrical conductivity of polymers.[1–9] One way to improve the thermal and electrical conductivity, as well as the viscoelastic behavior and mechanical properties, of these materials is to combine polymer matrices with highly conductive fillers. Several types of these fillers (metallic, graphitic, and other inorganic or organic fillers) in numerous shapes are commonly used as electrically and thermally conductive fillers.[10,11] However, metallic fillers have some disadvantages which limit their usage. Most metallic fillers have spherical shapes, which give rise to high percolation thresholds, and thus large filler fractions are necessary in the composite, increasing the price and weight of the material. Nanostructured expanded graphite (EG) sheets or platelets are light, anisotropic, and conductive.[10,12,13] These properties make EG nanoplatelets ideal fillers to achieve light and conductive polymer nanocomposites that can be useful for many industrial applications. The electrical conductivity of the nanocomposites is normally dominated by the interfacial interaction and network pathway contact points. Thus, the conductivity of EG nanocomposites should strongly depend on the surface properties of EG and the polymer–EG interface.

Many polymers reinforced with conductive fillers have been studied, but there are still many unsolved problems with respect

to calculations around particle sizes, shapes, concentrations, and the properties of each constituent. Some theoretical equations have been proposed to predict the electrical and thermal conductivities of polymeric materials. Only a few studies were dedicated to a comparative analysis of the electrical and/or thermal conductivities of two-phase systems.[2,3] Tlili *et al.*[2] reported on the thermal and electrical conductivities of EVA14 filled with EG and unexpanded graphite (UG). Their nanocomposites were prepared by melt mixing. They found that the thermal conductivity increased significantly with increasing EG content up to 0.82 W m^{-1} K^{-1}, while for UG it only increased up to 0.45 W m^{-1} K^{-1}. They also found an electrical percolation threshold of about 6 vol % for the EVA/EG composites (with a maximum electrical conductivity of 7.53×10^{-2} S cm^{-1}) and 17 vol % for the EVA/UG composites (with a maximum electrical conductivity of 5.05×10^{-4} S cm^{-1}). Tavman *et al.*[3] investigated the thermal diffusivity of conductive composites based on EVA14 filled with EG and UG. They used exactly the same preparation method and their observations were similar to those of Tlili *et al.*[2]

Modification of polymers and their composites by electron beam (EB) radiation can be used for many polymer processing applications including cross-linking, degradation, hardening, surface modification, and coating. According to literature, polymers may simultaneously undergo various reactions such as degradation, cross-linking, grafting, and oxidation during EB irradiation, depending on the irradiation dose and conditions.[14] The irradiation of polymers with ionizing radiation such as gamma rays, X-rays, accelerated electrons, and ion beams are of great importance to many processing applications.[15] The primary advantages of high-energy EB radiation are that it is pollution free, and has a high efficiency, low operation cost, room temperature operation, and the ability to process large throughputs.

High-energy electrons are used for cross-linking of polymeric materials in a wide range of applications such as cable and wire insulations, tubes, foams, heat shrinkable tubes, and shape memory products. High-energy electron induced cross-linking is mainly performed at ambient temperature and leads to the formation of three-dimensional networks. Due to these changes in polymer structure, an increase in chemical (increased resistance against solvents), mechanical (increased resistance against stress cracking corrosion), and thermal (increased resistance against thermal pressure) properties can be achieved.[14–16] Ethylene copolymers like EVA belong to polymers which can be cross-linked by high-energy electrons without any use of additional cross-linking agents. It is generally believed that the cross-linking starts by hydrogen elimination from the terminal methyl groups of the acetate side chain, which then reacts with other activated sites or methylene units of the main chain in a rather complex mechanism, including degradation reactions.[17,18]

Although there has been no study on the effect of EB irradiation on EVA/EG and/or EVA/SDS-EG composites, the effect of gamma irradiation on EVA-based composites was investigated.[19,20] Sen *et al.*[19] studied the effect of gamma irradiation in a nitrogen atmosphere on EVA13 and EVA13/carbon black composites prepared by a sol–gel method. Their samples were subjected to up to 400 kGy gamma rays at ambient conditions. They found that cross-linking and chain scission resulted from the gamma irradiation in nitrogen atmosphere. Khodkar *et al.*[20] investigated the effect of ^{60}Co γ-irradiation in the presence of air and nitrogen on EVA18/hollow fiber composites prepared by melt mixing in a co-extruder. They showed that this irradiation in nitrogen enhanced the mechanical and thermomechanical properties, while irradiation in air caused no changes in these properties. In comparison to EB irradiation, ^{60}Co γ-irradiation in air leads to more degradation of EVA due to lower dose rate and undesired reactions with oxygen.

This study involves a comparative analysis of the electrical and thermal conductivities, as well as thermal and mechanical properties, of nonirradiated and irradiated samples of EVA18 containing EG or SDS-EG. We are not aware of any other reported work on similar systems.

EXPERIMENTAL

Materials

Expanded graphite, SIGRAFLEX Expandat, was provided by the SGL Technologies GmbH, SGL Group. It has a conductivity of 20 S cm^{-1} (room temperature, 30 MPa, self-made 2-point conductivity tester, coupled with a DMM2000 Electrometer, Keithley Instruments), an apparent volume of ~400 cm^3, and a specific surface of 39.4 m^2 (77.4 K, N_2 atmosphere, Autosorb-1, Quantachrome). Ethylene vinyl acetate (EVA-460) was manufactured and supplied in granule form by DuPont Packaging & Industrial Polymers. EVA-460 contains 18% by weight of vinyl acetate (VA) with a BHT antioxidant thermal stabilizer. It has a melt flow index (190°C/2.16 kg) of 2.5 g/10 min (ASTM D1238-ISO 1133), a melting temperature of 88°C, a Vicat softening point of 64°C, and a density of 0.941 g cm^{-3}. The sodium lauryl sulphate known as sodium dodecyl sulphate (SDS) was supplied by Sigma-Aldrich and was used without further treatment.

METHODS

Preparation of Nanocomposites

Four grams of SDS was dissolved in 5 L deionized water in a glass beaker, and 20 g of the expanded graphite was gradually added to the solution. Suspensions of 500 mL were sonicated for 30 min with an ultrasound power of 500 W and a frequency of 20 kHz, filtered, washed with 100 mL distilled water to remove loosely adsorbed SDS, and dried in a vacuum oven at 50°C for 72 h. This modified EG, as well as the as-received unmodified EG, were mixed with EVA to prepare the nanocomposites. The EVA composites, with EG loadings of 0, 2, 4, 6, 8, and 10 wt %, were prepared by melt mixing using a Brabender Plastograph 55 mL internal mixer. The mixing was done for 15 min at 60 rpm and 100°C. The samples were melt-pressed at 100°C and 50 bar for 5 min into 2-mm-thick sheets by using a hot hydraulic press. For the thermal conductivity test, the samples were compression molded at 100°C and 50 bar for 5 min into 5-mm-thick cylindrical disks with a diameter of 12 mm. The filler amount in the composites was varied between 0 and 10 wt %.

Electron Beam Irradiation

All the EVA/EG and EVA/SDS-EG samples, packed in polyethylene bags filled with nitrogen in order to avoid oxygen-induced degradation, were irradiated with 1.5 MeV electrons using an electron accelerator ELV-2 (Budker Institute of Nuclear Physics, Novosibirsk, Russia) installed in the Leibniz Institute of Polymer Research Dresden.[21] A two-side irradiation was used in order to ensure a good dose uniformity. The absorbed dose amounted to 50 kGy and was applied at room temperature (25 ± 1°C) and at a beam current of 4 mA.

Characterization and Analysis

Scanning electron microscopy (SEM) analyses was carried out in a TESCAN VEGA3 Superscan scanning electron microscope (Brno, Czech Republic). The fracture surfaces of the samples were coated with gold to prevent static charges during analysis. Microscope settings of 285.5 nm probe size, 50 mA probe current, and 30 kV AC voltage were used.

The gel content of the samples was determined using Soxhlet solvent extraction. Rectangular test specimens with masses of approximately 0.2 g were wrapped in a 120 fine mesh stainless-steel cage and refluxed with xylene at 140°C for about 12 h and then dried at 80°C under vacuum overnight to determine the gel fraction. The gel content values were averaged over at least 2 tests and calculated according to eq. (1).

$$\text{Gel content } (\%) = \left(1 - \left[\frac{(m_{BE} - m_{AE})}{(1-F)(m_{BE})}\right]\right) \times 100\ \% \qquad (1)$$

where m_{BE} is the sample mass before extraction; m_{AE} is the sample mass after extraction; F is the fraction of filler insoluble in xylene in the composites.

The volume resistance measurements of the samples were carried out on a 6157A Keithley Instruments electrometer, connected to an 8009 Keithley Resistivity Test Fixture with two-plate electrodes located on both sides of the samples. This method is appropriate for resistance values in the range of $10^7 - 10^{18}$ Ω at room temperature in accordance with ASTM D257-07. The corresponding conductivity values are in the range of 10^{-19} to 10^{-8} S cm^{-1}, but sensible results can be found in the range of 10^{-19} to 10^{-4} S cm^{-1}.

The thermal conductivity measurements were done using a Hot Disc Thermal Constant Analyser TPS 500 (Sweden) at room temperature (24°C). The measurement system is based on the transient plane source technique. The sensor is sandwiched between two pieces of sample having cylindrical shapes with 12 mm diameter and 5–6 mm height. The sensor used has a radius of 3.189 mm and the measurement time was 2.5 s with a heating power of 2.048 W. The measurements were done on both surface sides of the nonirradiated system. For the irradiated samples, the sensor was placed between two sample films on top of cylindrical pieces protected with insulator material. The device measures the thermal conductivity (λ), thermal diffusivity (α), and the specific heat capacity (C_p). The material density (ρ_{th}) was determined by the rule of mixtures (eq. (2)) using a density of 0.941 g cm^{-3} for EVA and 2.25 g cm^{-3} for EG,[9] where ρ_{EVA}, ρ_{EG}, and φ are the density of EVA, expanded graphite, and the filler volume fraction, respectively. By using eq. (3), the theoretical thermal conductivity (λ) can be readily calculated.[1–3]

$$\rho_{th} = \rho_{EVA}(1-\varphi) + \rho_{EG}\varphi \qquad (2)$$

$$\lambda = \alpha.\ \rho.\ C_p \qquad (3)$$

DSC analyses were carried out under nitrogen flow (20 mL min^{-1}) using a Perkin Elmer Pyris-1 differential scanning calorimeter (Waltham, Massachusetts, USA). The instrument was calibrated using the onset temperatures of melting of indium and zinc standards, as well as the melting enthalpy of indium. Three samples of 5–10 mg for each composition were analyzed in the temperature range from 25 to 180°C in a heating–cooling–heating cycle at a rate of 10°C min^{-1}. For all the samples, the onset and peak temperatures of melting and crystallization, as well as the melting and crystallization enthalpies, were determined from the first heating and cooling scans. The normalized enthalpies of melting and crystallization in Table I were determined from eq. (4).

$$\Delta H_m^{Norm} = \frac{\Delta H_{m,EVA}}{w_{EVA}} \qquad (4)$$

where $\Delta H_{m,EVA}$ is the experimentally observed melting enthalpy for the pure EVA and ΔH_m^{Norm} is the calculated normalized enthalpy of melting for EVA with a weight fraction w_{EVA} in the composite. The degree of crystallinity χ_c was calculated from eq. (5).

$$\chi_c = (\Delta H_m^{Norm}/\Delta H_m^o) \times 100\ \% \qquad (5)$$

where ΔH_m^o is the specific enthalpy of melting for 100% crystalline PE. A value of 288 J g^{-1} was used in the calculations.[16,19,20] The enthalpy of melting of polyethylene (PE) was used to calculate the degree of crystallinity of EVA, since there is no data

Table I. TGA Results for All the Irradiated Samples

wt. % EG	$T_{10\%}$ (°C)	T_{max} (°C)	Weight % residue
No SDS modification			
0	352.7	465.4	0
2	357.7	464.7	1.8
4	351.1	465.1	3.5
6	353.0	466.0	5.2
8	353.7	464.7	7.8
10	350.1	459.1	9.1
SDS modification			
0	352.7	465.4	0
2	359.5	473.5	2.7
4	354.7	462.7	3.5
6	354.2	465.2	6.0
8	352.0	466.0	7.6
10	349.2	468.2	8.1

$T_{10\%}$ and T_{max} are the degradation temperatures at 10% mass loss and maximum mass loss rate, respectively.

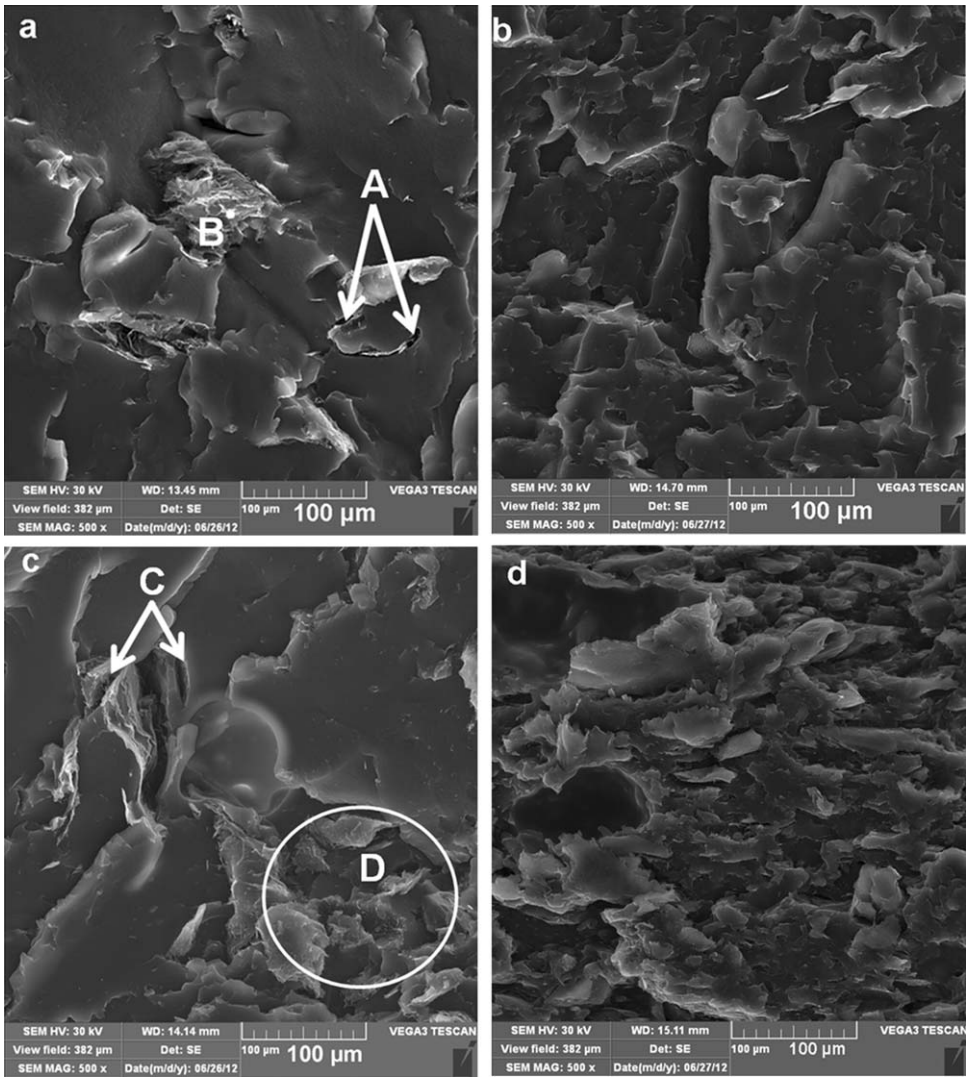

Figure 1. SEM micrographs of irradiated EVA/EG composites: (a) 98/2 w/w EVA/EG; (b) 98/2 w/w EVA/SDS-EG; (c) 90/10 w/w EVA/EG; (d) 90/10 w/w EVA/SDS-EG.

available on the enthalpy of 100% crystalline EVA, and since only the PE segments, that form the backbone of EVA, crystallize.

Thermogravimetric analysis (TGA) was done under flowing nitrogen (20 mL min^{-1}) using a Perkin Elmer Pyris-1 thermogravimetric analyzer (Waltham, Massachusetts, USA). The samples, weighing ~20 mg each, were heated from 30 to 600°C at a heating rate of 10°C min^{-1}.

Tensile testing was performed under ambient conditions on a Hounsfield H5KS universal tester at a cross-head speed of 50 mm min^{-1}. The specimens were dumbbell shaped (gauge length 20 mm, width 2 mm, and thickness 2 mm) and analyzed according to ASTM D19671. The tensile modulus as well as stress and elongation at break of the samples were calculated from the stress–strain curves. At least five specimens were tested for each sample and the mean values and standard deviations are reported.

RESULTS AND DISCUSSION

Scanning Electron Microscopy (SEM)

The SEM micrographs of the fracture surface of the irradiated EVA nanocomposites filled with 2 and 10 wt % EG and SDS-EG are shown in Figure 1. It can be seen that there are some agglomerates (position B) and cracks (positions A and C) along the interface in the irradiated EVA/EG samples [Figure 1(a,c)]. This indicates that there was interfacial debonding between the EG platelets and EVA. As the filler content increased to 10 wt %, EG clusters are observed [position D in Figure 1(c)]. In our previous work[22] on nonirradiated composites, the SEM images showed big particle agglomerations of the EG present in the materials prepared without any dispersing agent. The explanation was that the EG sheets tend to agglomerate and are more difficult to disperse in the matrix because of insufficient shear force to break down the EG agglomerates.

Although not very clear, it seems as if the SDS-EG sheets were more uniformly dispersed in the matrix of the irradiated

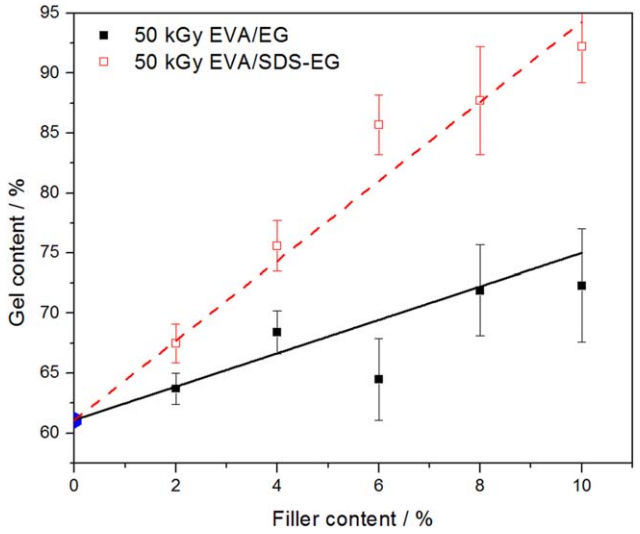

Figure 2. Gel content as function of EG content for irradiated samples without and with SDS treatment. [Color figure can be viewed in the online issue, which is available at wileyonlinelibrary.com.]

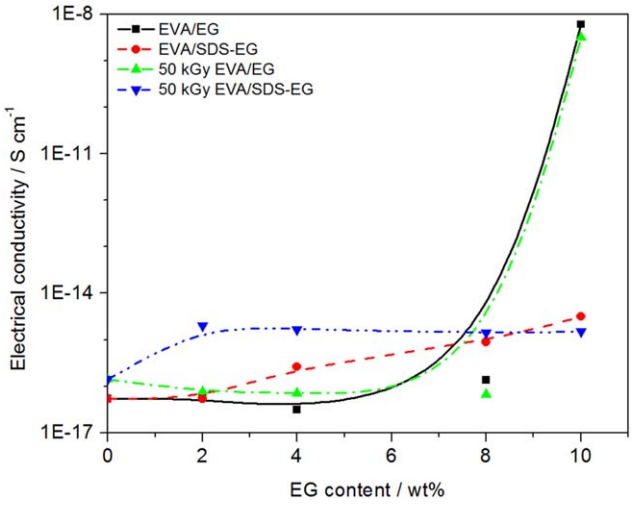

Figure 3. Electrical conductivity of EVA composites without and with surfactant modification and electron radiation. [Color figure can be viewed in the online issue, which is available at wileyonlinelibrary.com.]

composites due to the effect of surfactant treatment in enhancing the interfacial adhesion [Figure 1(b,d)]. There are no obvious voids at the boundaries between the two components, confirming that the pores of the EG are effectively impregnated with EVA. In an investigation of optimal conditions for the dispersion of SDS-treated carbon nanotubes (CNT), it was found that SDS becomes ineffective at lower or higher concentrations than a certain optimal concentration, because the SDS either does not properly coat the CNT surfaces, or forms micelles when it exceeds the critical micelle concentration which also reduces its ability to properly cover the CNT surfaces.[23] We did not specifically investigate the influence of SDS concentration on the EG dispersion in our polymer, but all the experimental results presented in this article indicate improved dispersion of the EG after SDS treatment. After EB irradiation, the surface morphology of the samples [Figure 1(b,d)] did not change compared to the nonirradiated EG and SDS-EG composites.[22] This indicates that there was no EVA melting at a macroscopic level when the EB penetrated the polymer, and the EG or SDS-EG particles could not rearrange. Similar observations were reported by Dubey *et al.*[24] in their study of radiation-processed EVA reinforced with MWCNT prepared *via* melt mixing. They observed homogeneity in all their samples and no agglomerations of MWCNT in the investigated composition range. This was attributed to the better interfacial interactions and good compatibility between the components induced by multifunctional acrylates (antioxidants). These multifunctional acrylates were introduced to the system to overcome the deterioration of mechanical properties of EVA at high radiation dose.

Gel Content

The dependence of gel content of the irradiated EVA on the EG and SDS-EG contents is shown in Figure 2. The nonirradiated EVA was completely soluble in hot xylene. The gel contents are accepted as a measure of the cross-linking density in EVA. An increase in gel content will cause a decrease in solubility due to the formation of three-dimensional networks in the irradiated polymer.[14,15] Since the radiation-induced cross-linking reactions normally occur primarily in the amorphous phase of the polymer,[25–30] the EB irradiation will induce cross-linking and some degradation in the amorphous phase, while the crystalline phase should not be affected.

The gel contents of all the samples increased with an increase in EG loading because of increased formation of insoluble macromolecular networks (cross-links) in the polymer. The EG obviously conducts energy from the EB irradiation and improves the efficiency of free radical formation and cross-linking. The irradiated SDS-EG containing composites have significantly higher gel content values than the irradiated EG samples. This is probably due to the improved interaction and dispersion of the EG platelets in the EVA, which further improved the energy transfer to the EVA chains and the resultant cross-linking efficiency.

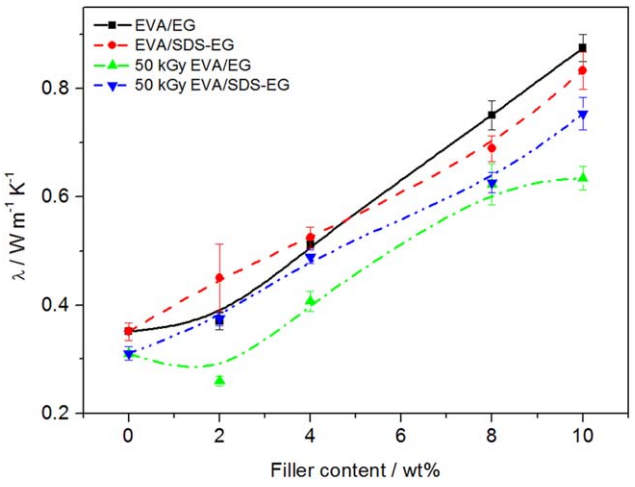

Figure 4. Thermal conductivity of EVA/EG composites in the absence and presence of SDS and radiation treatment. [Color figure can be viewed in the online issue, which is available at wileyonlinelibrary.com.]

Table II. Thermal Conductivities of Nonirradiated and Irradiated EVA Samples

	Nonirradiated samples		Irradiated samples	
wt % EG	$\lambda_{EVA/EG}$ (W m^{-1} K^{-1})	$\lambda_{EVA/SDS-EG}$ (W m^{-1} K^{-1})	$\lambda_{50\ kGy\ EVA/EG}$ (W m^{-1} K^{-1})	$\lambda_{50\ kGy\ EVA/SDS-EG}$ (W m^{-1} K^{-1})
0	0.351 ± 0.017	0.351 ± 0.017	0.310 ± 0.013	0.310 ± 0.013
2	0.370 ± 0.015	0.450 ± 0.062	0.259 ± 0.008	0.375 ± 0.012
4	0.511 ± 0.006	0.524 ± 0.019	0.407 ± 0.018	0.489 ± 0.013
6	0.654 ± 0.011	0.657 ± 0.035	0.484 ± 0.009	0.447 ± 0.010
8	0.750 ± 0.027	0.689 ± 0.024	0.623 ± 0.038	0.626 ± 0.019
10	0.877 ± 0.025	0.833 ± 0.035	0.634 ± 0.022	0.753 ± 0.030

$\lambda_{EVA/EG}$, $\lambda_{50kGy\ EVA/EG}$, $\lambda_{EVA/SDS-EG}$, and $\lambda_{50kGy\ EVA/SDS-EG}$ are the thermal conductivities of the EVA/EG, irradiated EVA/EG, EVA/SDS-EG, and irradiated EVA/SDS-EG composites, respectively.

Electrical Conductivity

Figure 3 shows the electrical conductivities of all the investigated samples as a function of EG content. It is evident that the EVA/EG composites with and without radiation had a percolation threshold of about 8 wt %. EB radiation did not have any effect on the electrical conductivities of the composites. In the case of the composites containing SDS-EG, there was no conductivity, even at an SDS-EG filling of 10 wt % (9.5% actual EG content), independent of irradiation. Possible reasons for this observation are that (i) the presence of SDS separates the EG platelets so effectively that percolation pathways will only be formed at much higher SDS-EG contents and (ii) the SDS forms an isolating layer around the EG platelets which reduces their effective electrical conductivity.

Thermal Conductivity

The thermal conductivity of EVA and its composites in the absence and presence of SDS, and without or with irradiation treatment, are presented in Figure 4 and summarized in Table II. An increase in the thermal conductivity with increasing filler content was observed for all the investigated samples. This is due to the fact that the filler has a much higher thermal conductivity (6.0 W m^{-1} K^{-1})[29] than EVA (0.35 W m^{-1} K^{-1}). The nonirradiated composites containing EG and SDS-EG have very similar thermal conductivities within experimental error. A number of factors, such as dispersion of EG sheets, matrix crystallinity, and crystal structure, degree of interfacial thermal contact between the components, and scattering of phonons contribute to the thermal conductivities of such composites. Scattering of phonons at the EG/polymer interface and at the EG/EG contact sites may suppress heat conduction in the composites, and the surfactant itself may have an insulating effect, while the improved dispersion of the EG may increase the thermal conductivity, especially when continuous EG paths are formed. However, a percolation phenomenon is not observed in contrast to the findings on electrical conductivity (compare with Figure 3). This difference between the electrical and thermal conductivity is due to a different mechanism of electron transport (allowing electron hopping over a few nanometers from filler particle to filler particle) and phonon transport (scattering at interfaces in heterogeneous systems). Since the crystallinities in the EVA/SDS-EG composites are higher than those in the corresponding SDS-free composites,[22] which could count for higher thermal conductivities, one can only speculate about the similarity of the thermal conductivities in the two composite systems. The finer morphology of the EVA/SDS-EG composites with higher numbers of interfaces probably counterbalances the effect of higher crystallinity.

The nonirradiated EVA/EG composites have higher thermal conductivity values than the irradiated EVA/EG samples. This is surprising since in the nonirradiated samples, the crystallinity decreased with increasing EG content,[22] while it increased in the irradiated samples (Figure 6). The cross-linking in the irradiated composites probably induced restricted chain mobility and reduced vibration of phonons, which hampered the heat transfer and led to lower conductivities. The changes in interstitial spaces induced by irradiation also contributed toward fewer vibrational modes which resulted in lower thermal conductivities.[29] The irradiated SDS-EG containing composites also show lower thermal conductivities than the nonirradiated ones, but the difference is not as big as in the case of the EG composites. This is probably the result of the relatively high crystallinity in

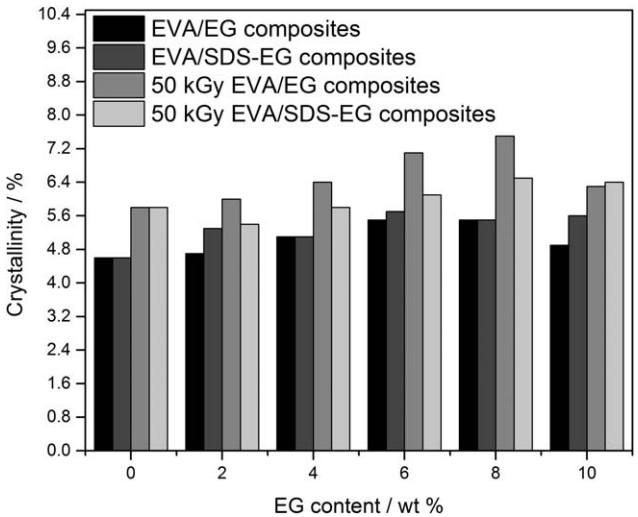

Figure 5. Crystallinities of nonirradiated and irradiated EVA and its composites with and without SDS as a function of EG content.

Table III. Data Obtained from the First Heating and Cooling DSC Curves of All the Irradiated Samples

wt % EG	$T_{p,m}$ (°C)	$T_{p,c}$ (°C)	ΔH_m (J g^{-1})	ΔH_m^{Norm} (J g^{-1})	χ_c (%)
No modification					
0	84.8 ± 0.8	62.6 ± 0.1	16.7 ± 0.4	16.7	5.8
2	84.4 ± 0.7	62.1 ± 0.2	17.0 ± 0.5	17.3	6.0
4	84.2 ± 0.5	61.8 ± 1.4	17.6 ± 0.7	18.3	6.4
6	84.3 ± 0.1	61.3 ± 0.8	19.3 ± 0.1	20.5	7.1
8	83.4 ± 0.3	61.7 ± 1.3	20.0 ± 3.4	21.7	7.5
10	83.1 ± 0.3	61.5 ± 1.2	16.4 ± 0.1	18.2	6.3
SDS modification					
2	84.3 ± 0.4	62.3 ± 0.3	15.3 ± 0.1	15.6	5.4
4	84.2 ± 0.4	62.2 ± 0.1	16.1 ± 0.7	16.8	5.8
6	83.6 ± 0.3	62.0 ± 0.2	16.5 ± 0.6	17.6	6.1
8	83.9 ± 0.7	61.7 ± 0.6	17.1 ± 0.1	18.6	6.5
10	83.8 ± 0.2	61.7 ± 1.0	16.6 ± 1.2	18.4	6.4

$T_{p,m}$ is the peak temperature of melting; $T_{p,c}$ is the peak temperature of crystallization; ΔH_m is the measured melting enthalpy; ΔH_m^{Norm} is the normalized melting enthalpy of EVA18 taking into account its mass fraction; χ_c is the EVA18 crystallinity in the samples.

the irradiated samples[22] (Figure 6), and of the more intimate contact between the EVA and EG in the presence of SDS, even in the absence of irradiation and cross-linking. Both these effects partially balance the negative effect of restricted chain mobility due to cross-linking.

Differential Scanning Calorimetry (DSC)

The crystallinity of the EVA originates from the polyethylene segments and is directly proportional to the melting enthalpy. The DSC data for the first heating run of all the nonirradiated and irradiated samples are shown in Figure 5, and reflect changes in the crystalline structure after EB irradiation. The melting enthalpy values were normalized to the mass content of EVA in the samples (Table III). The crystallinities of the nonirradiated samples increased slightly with increasing EG content up to 6 wt %, after which it slightly decreased. It seems as if at lower EG contents the nucleation effect of the EG particles on the polymer chains was more dominant than the immobilization effect, while the immobilization effect became more dominant at higher EG contents where there was probably more agglomeration. The irradiated samples showed the same trend, but their crystallinities are observably higher than those of the comparable nonirradiated samples. The reason is probably that, because of chain scission and localized melting induced by the EB irradiation, some recrystallization occurred and the shorter chain segments rearranged into a more crystalline morphology.

The melting and crystallization temperatures of EVA in the irradiated samples did not really change within experimental error in the presence of EG and SDS-EG and with increasing EG content (Table III). These values are, however, slightly lower than those of the nonirradiated samples, where the melting temperatures varied between 84.1 and 85.4°C and the crystallization temperatures between 65.0 and 66.7°C. The lower melting temperature is a sign of less perfect or smaller crystallites. This is certainly caused by hindered chain mobility during crystallization due to the cross-linked structure, which normally causes lower crystallization temperatures in cross-linked systems.

Thermogravimetric Analysis

Figures 6(a) and 7(a) show a comparison of the thermal stabilities of nonirradiated and irradiated EVA/EG and EVA/SDS-EG composites. The TGA curves of the irradiated EVA and its irradiated composites in the absence and presence of SDS treatment are shown in Figures 6(b) and 7(b). Table I summarizes the degradation temperatures at 10% mass loss and at the maximum mass loss rate of these samples. It is generally accepted that the first mass loss step between 350 and 400°C is due to deacetylation with β-elimination of the acetic acid and the formation of carbon–carbon double bonds along the polymer backbone. The results in Figures 6 and 7 and Table I show that less acetic acid is evolved between 350 and 400°C for the irradiated samples, probably because of cross-linking taking place in the amorphous phase which consists mainly of VA monomers. This cross-linking restricted the chain mobility and also the mobility of the free radicals formed during thermal degradation. The degradation of the main chain at about 475°C was faster for the irradiated samples, which may be due to some degradation of the EVA chains and formation of additional free radicals from tertiary main chain carbons introduced by the EB radiation.[17] The temperature values in Table I vary within a 10°C bracket, but there is no trend and the thermal stability of the irradiated composites is comparable to that of the irradiated EVA. Our previous work[22] shows a clear improvement in thermal stability in the presence of EG and SDS-EG, and with increasing filler content.

Figures 6(b) and 7(b) show that the degradation of the main chain started even before the end of the deacetylation step for the EG and SDS-EG samples, and the onset of second-step degradation decreases with increasing filler content. The most probable reason for this is the more effective initiation of degradation during irradiation when EG or SDS-EG is present in the

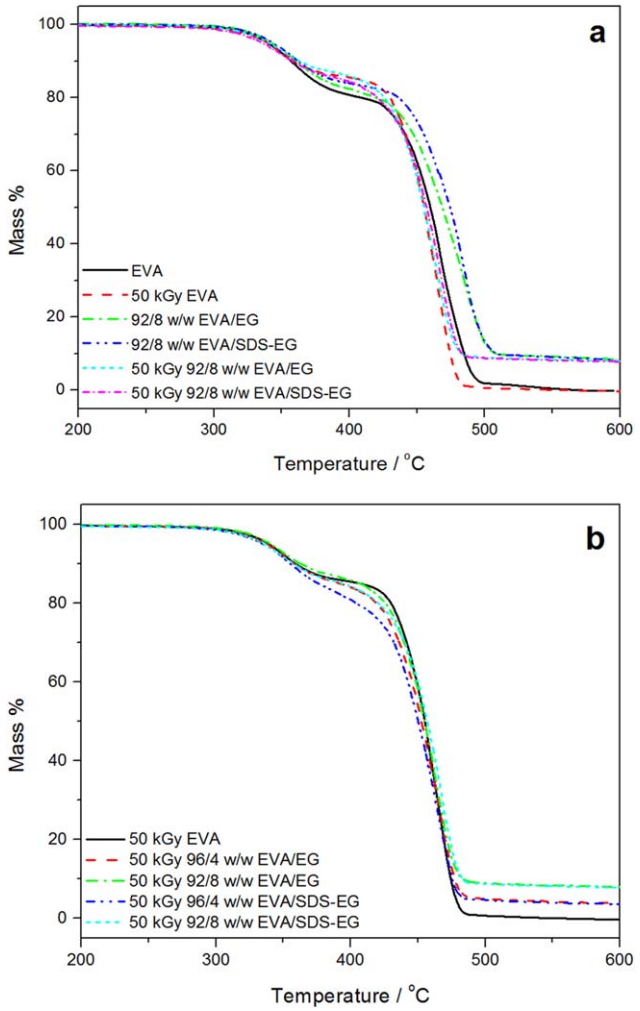

Figure 6. TGA curves of nonirradiated and irradiated (a) EVA/EG and (b) EVA/SDS-EG composites. [Color figure can be viewed in the online issue, which is available at wileyonlinelibrary.com.]

samples. As mentioned before, these fillers probably transport heat energy more effectively through the sample, improving the thermal degradation during irradiation. The percentage residues of all the composites correlate well with the EG contents initially mixed into the EVA matrix, indicating good dispersion of the filler in the polymer.

Tensile Properties

Composites with good mechanical properties can be obtained when the graphite platelets are well dispersed in the EVA matrix, and when there is good interaction between the polymer and the filler. From previously discussed results, we know that the presence of SDS improves the interaction between EVA and EG, and the dispersion of EG in the EVA matrix. The EB irradiation treatment induces cross-linking which should contribute to improving the mechanical properties of the composites, not only because of network formation but also because of trapping the EG platelets in the formed network.

Figure 8 shows that the tensile stress at break is generally reduced in the presence of and with increasing EG content. As is generally known and also explained in our previous article,[22] inorganic filler in a polymer normally forms defect centers at which crazes and cracks start forming when stress is applied to the sample. The propagation of the cracks gives rise to sample fracture. For the nonirradiated samples, the results in Figure 8 clearly show higher stress at break values for the EVA/SDS-EG composites, and we explained this observation in our previous article[22] as being the result of the higher extent of agglomeration of the EG particles in the EVA/EG composites, which resulted in the crazes formed during stretching more easily developing into cracks that lead to fracture at lower stresses. The EVA/SDS-EG systems have smaller and better dispersed EG particles that are closer to each other, and therefore, it is more difficult for cracks to develop, because a growing craze which started at one particle may terminate at another particle before it develops into a crack. More strain energy is therefore needed for crack development and growth, so that fracture occurs at higher stress values. The irradiated EVA has a significantly higher value than the nonirradiated EVA, which is to be expected because of the formation of a cross-linked network. It is interesting that the nonirradiated SDS-EG containing samples

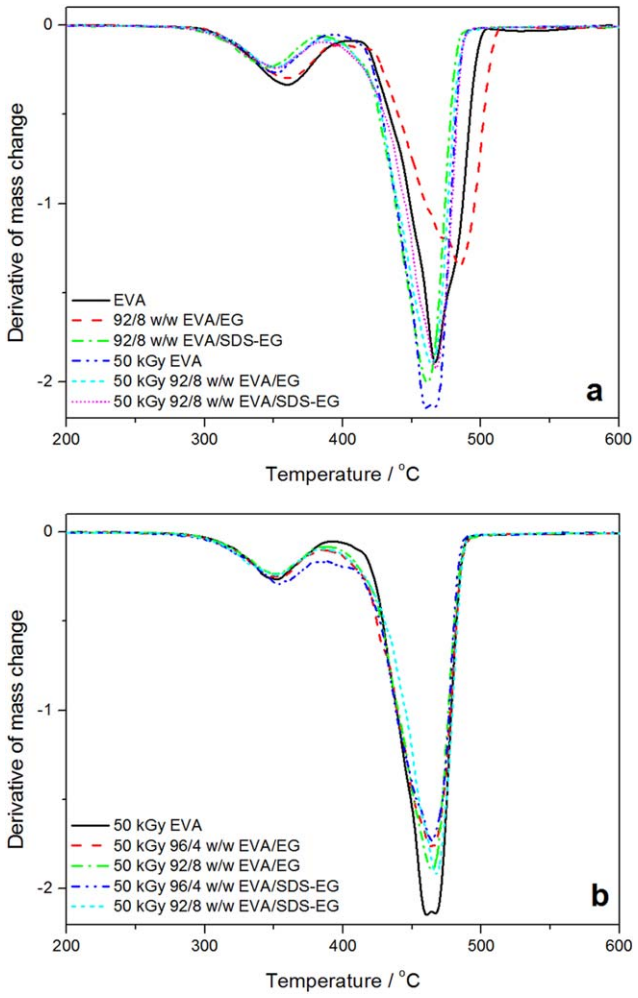

Figure 7. Derivative TGA curves of nonirradiated and irradiated (a) EVA/EG and (b) EVA/SDS-EG composites. [Color figure can be viewed in the online issue, which is available at wileyonlinelibrary.com.]

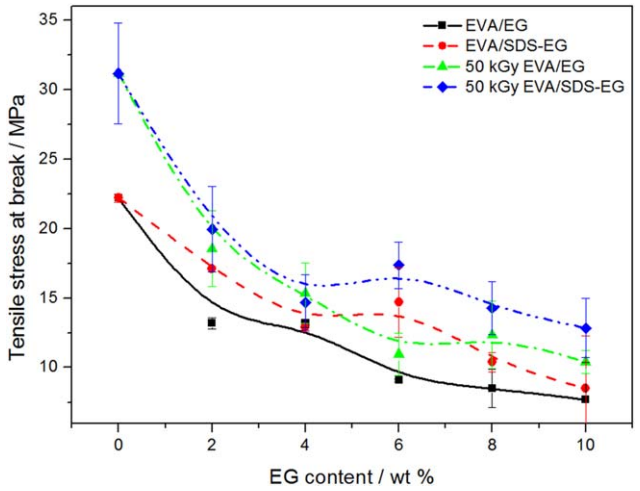

Figure 8. Variation of stress at break of nonirradiated and irradiated EVA/EG and EVA/SDS-EG samples as a function of filler content. [Color figure can be viewed in the online issue, which is available at wileyonlinelibrary.com.]

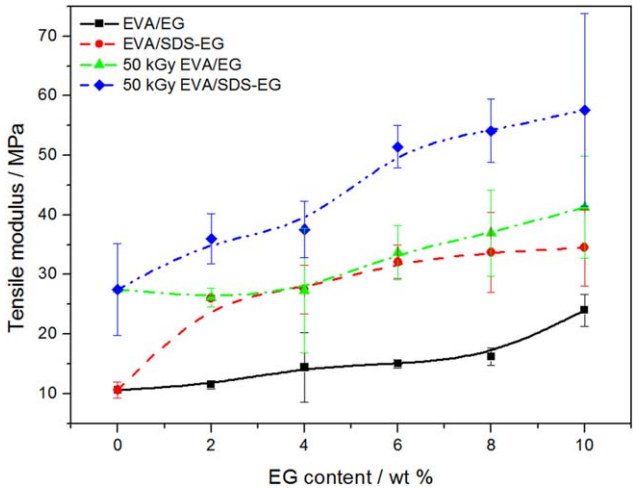

Figure 10. Variation of tensile modulus of nonirradiated and irradiated EVA/EG and EVA/SDS-EG samples as a function of filler content. [Color figure can be viewed in the online issue, which is available at wileyonlinelibrary.com.]

have about the same stress at break values than the irradiated EG containing samples within experimental error. It seems that the improved interaction and dispersion of the filler particles has the same effect on the stress at break of the composite than the network formation as a result of radiation-induced cross-linking of the polymer matrix. However, the improved interaction and dispersion combined with the radiation-induced cross-linking give even better stress at break values, which is important when one wants to improve the thermal properties without sacrificing too much on the tensile properties. Unfortunately, the electrical conductivity of the samples treated in this way remains very low up to a filler content of 10 wt %.

The elongation at break of the EVA observably increased after EB irradiation (Figure 9), which is the result of the cross-linked network formation. The elongation at break values of the composites containing the same amount of EG, however, are very similar within experimental error, independent of surfactant and/or radiation treatment. In these samples, there is a complex combination of many factors that contribute to the mechanical stability of the samples. The fracture mechanism of composites will be influenced by cross-linking, but it will be dominated by the dispersion of the filler particles and the interaction between the polymer and the filler particles. This is the reason why the EB irradiated composites show elongation at break values very similar to those of the nonirradiated composites. From Figure 9, it is, however, clear that the SDS-EG containing samples gave slightly better elongation at break values, which is in line with the better stress at break values discussed above, and which is the result of the improved dispersion of SDS-EG compared to that of EG.[22]

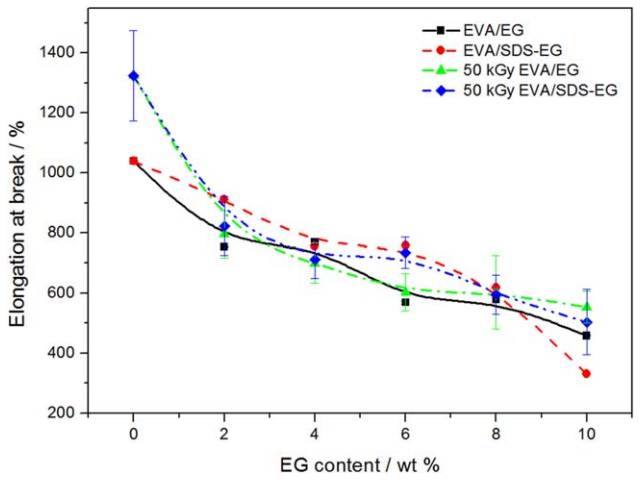

Figure 9. Variation of elongation at break of nonirradiated and irradiated EVA/EG and EVA/SDS-EG samples as a function of filler content. [Color figure can be viewed in the online issue, which is available at wileyonlinelibrary.com.]

The tensile modulus of the composites generally increased with increasing filler content (Figure 10), which is to be expected because of the high modulus of the EG filler. Like the stress at break, the modulus of EVA increased after EB irradiation of the sample because of the radiation-induced formation of a cross-linked network. As was observed in the stress at break results, the nonirradiated EVA/SDS-EG samples have modulus values very similar to those of the irradiated EVA-EG samples. The improved interaction and dispersion as a result of SDS treatment result in a similar improvement in composite stiffness than the cross-linking of the polymer matrix. It is further clear from Figure 10 that SDS treatment and EB irradiation has an additive effect on the improvement of the tensile modulus, with more than 100% increase in tensile modulus compared to the untreated EVA/EG composites.

CONCLUSIONS

The effect of the surfactant and radiation treatment on the thermal and mechanical properties, as well as electric and thermal conductivities, of EVA18/EG nanocomposites was investigated. The SDS treatment of EG clearly improved the interaction

between EVA and EG and the dispersion of EG in the polymer matrix. EB irradiation-initiated cross-linking formed a network in the amorphous part of EVA, and the gel content increased with increasing filler content in EVA. This increase was more significant for the SDS-EG containing samples. However, improved interaction between the filler and the polymer due to irradiation was not found. The improved dispersion of EG due to SDS treatment, the network formation due to EB irradiation, and the combination of these two effects significantly influenced the tensile properties of the composites, improving the modulus and the stress at break of the composites. The thermal properties showed little change as a result of EB irradiation, probably because irradiation mostly affected the amorphous parts of the polymer. The irradiation had very little effect on the electrical conductivities of the composites, while the thermal conductivities of the irradiated composites were generally slightly lower than those of the comparable nonirradiated composites.

ACKNOWLEDGMENTS

This work was financially supported by the National Research Foundation of South Africa (UID 73982) and the International Bureau of the BMBF in Germany (project SUA 10/009).

REFERENCES

1. Kochetov, R.; Korobko, A. V.; Andritsch, T.; Morshuis, P. H. F.; Picken, S. J. *Journal of Physics D: Applied Physics* **2011**, *44*, 1.
2. Tlili, R.; Boundenne, A.; Cecen, V.; Ibos, L.; Krupa, I.; Candau, Y. *International Journal of Thermophysics* **2010**, *31*, 936.
3. Tavman, I. H.; Turgut, A.; da Fonseca, H. M.; Orlande, H. R. B.; Cotta, R. M.; Magalhaes, M. *International Journal of Thermophysics* **2013**, *34*, 2297.
4. Carotenuto, G.; De Nicola, S.; Palomba, M.; Pullini, D.; Horsewell, A.; Hansen, T. W.; Nicolais, L. *Nanotechnology* **2012**, *23*, 1.
5. Yasmin, A.; Luo, J.-J.; Daniel, I. M. *Composites Science and Technology* **2006**, *66*, 1179.
6. Bhattacharya, S.; Tandon, R. P.; Sachdev, V. K. *Journal of Materials Science* **2009**, *44*, 2430.
7. Konwer, S.; Dolui, S. K. *Materials Chemistry and Physics* **2010**, *124*, 738.
8. Weng, W.-G.; Chen, G.-H.; Wu, D.-J.; Yan, W.-L. *Composite Interfaces* **2004**, *11*, 131.
9. Piana, F.; Pionteck, J. *Composites Science and Technology* **2013**, *80*, 39.
10. Goyal, R. K.; Samant, S. D.; Thakar, A. K.; Kadam, A. *Journal of Physics D: Applied Physics* **2010**, *43*, 1.
11. Kim, S.; Do, I.; Drzal, L. T. *Polymer Composites* **2010**, *31*, 755.
12. Lee, J. H.; Shin, D. W.; Makotchenko, V. G.; Nararov, A. S.; Fedorov, V. E.; Yoo, J. H.; Yu, S. M.; Choi, J.-Y.; Kim, J. M.; Yoo, J.-B. *Small* **2010**, *6*, 58.
13. Stankovich, S.; Dikin, D. A.; Piner, R. D.; Kohlhaas, K. A.; Kleinhammes, A.; Jia, Y.; Wu, Y.; Nguyen, S. T.; Ruoff, R. S. *Carbon* **2007**, *45*, 1558.
14. Jing, J.; Chen, S.; Zhang, J. *Journal of Polymer Research* **2010**, *17*, 827.
15. Chen, S.; Zhang, J.; Sun, J. *Journal of Applied Polymer Science* **2009**, *114*, 3110.
16. Kim, S. R.; Poostforush, M.; Kim, J. H.; Lee, S. G. *eXPRESS Polymer Letters* **2012**, *6*, 476.
17. Matsui, T.; Shimoda, M.; Osajima, Y. *Polymer International* **1992**, *29*, 91.
18. Hirschl, Ch.; Biebl-Rydlo, M.; DeBiasio, M.; Mühleisen, W.; Neumaier, L.; Scherf, W.; Oreski, G.; Eder, G.; Chernev, B.; Schwab, W.; Kraft, M. *Solar Energy Materials & Solar Cells* **2013**, *116*, 303.
19. Şen, M.; Copuroğlu, M. *Materials Chemistry and Physics* **2005**, *93*, 154.
20. Khodkar, F.; Ebrahimi, N. G. *Journal of Applied Polymer Science* **2011**, *119*, 2085.
21. Dorschner, H.; Lappan, U.; Lunkwitz, K. *Nuclear Instruments and Methods in Physics Research B* **1998**, *139*, 495.
22. Sefadi, J. S.; Luyt, A. S.; Pionteck, J. *Journal of Applied Polymer Science* **2015**, *132*, 41352.
23. Shi, Y.; Ren, L.; Li, D.; Gao, H.; Yang, B. *Journal of Surface Engineered Materials and Advanced Technology* **2013**, *3*, 6.
24. Dubey, K. A.; Bhardwaj, Y. K.; Chaudhari, C. V.; Kumar, V.; Goel, N. K.; Sabharwal, S. *eXPRESS Polymer Letters* **2009**, *3*, 492.
25. Hwang, T. Y.; Lee, S.; Kang, P.-H.; Park, K. H.; Ahn, Y.; Lee, J. W. *Macromolecular Research* **2011**, *19*, 1151.
26. Osman, H.; Ismail, H.; Mariatti, M. Electron-beam irradiation of recycled newspaper filled polypropylene/natural rubber composites: Effect of crosslink promoters. ICCM-17 conference proceedings, Edinburgh, UK, 27–31 July **2009**.
27. Dadbin, S.; Frounchi, M.; Haji-Saeid, M.; Gangi, F. *Journal of Applied Polymer Science* **2002**, *86*, 1959.
28. Hassanpour, S.; Khoylou, F.; Jabbarzadeh, E. *Journal of Applied Polymer Science* **2003**, *89*, 2346.
29. Dadbin, S.; Frounchi, M.; Sabet, M. *Polymer International* **2005**, *54*, 686.
30. Hwang, T. Y.; Lee, S.; Kang, P.-H.; Park, K. H.; Ahn, Y.; Lee, J. W. *Macromolecular Research* **2011**, *19*, 1151.